International Journal of
INTELLIGENT SYSTEMS AND APPLICATIONS IN ENGINEERING
ISSN:2147-6799 www.ijisae.org Original Research Paper

Wireless Brain Implants for Neurological Disorder Treatment

[1]Rayudu Vinay Kumar, [2]Matta Venkata Durga Pavan Kumar, [3]Mamatha B, [4]Akkisetti Vn Hanuman

Submitted: 12/05/2023 **Revised:** 15/07/2023 **Accepted:**05/08/2023

Abstract: Brain implants, referred to as neural implants or neuroprosthetics, represent a compelling domain of investigation within neuroscience and biomedical engineering. These groundbreaking technologies has the potential to transform our comprehension of the brain and provide new opportunities for augmenting neuronal functioning. Brain implants, by directly connecting with the cerebral circuitry, have many uses, such as restoring sensory functioning and enhancing cognitive capacities. This article examines the progress of brain implants and its possible effects on human capacities and welfare. Keywords: Cerebral implants • Neuroprosthetics • Neural interfaces • Cognitive augmentation • Deep brain stimulation
Preface Progress in neuroscience and technology has resulted in revolutionary developments in brain implant technology. These implants, referred to as neuroprosthetics or neural interfaces, has the potential to transform our understanding of the human brain and provide many opportunities for addressing neurological illnesses, augmenting cognitive functions, and facilitating direct connections between our brains and machines. This article examines brain implants, focusing on their present uses, future possibilities, ethical issues, and societal effect. Comprehending cerebral implants Brain implants are electrical devices surgically inserted into the brain to monitor or stimulate neural activity. They include a series of microelectrodes that connect with neurons, facilitating bidirectional communication between the brain and external equipment. These implants serve several tasks, including the restoration of lost sensory or motor capabilities, the treatment of neurological illnesses, and the enhancement of cognitive capacities. Utilizations in medical science A prominent use of brain implants is within the domain of medical science. Neuroprosthetics have shown encouraging outcomes in reinstating functioning for persons with spinal cord injuries, allowing them to recover movement and autonomy. These implants provide new conduits for information transfer between the brain and the body by circumventing impaired neuronal connections. Furthermore, cerebral implants provide optimism for those afflicted with neurodegenerative conditions such as Parkinson's disease and epilepsy. Deep Brain Stimulation (DBS) implants may transmit electrical impulses to targeted brain areas, therefore mitigating symptoms and enhancing patients' quality of life. Responsive Neurostimulation implants identify atypical cerebral activity and provide precise stimulation to avert seizures. Reestablishing sensory functions Neural implants have shown encouraging outcomes in rehabilitating sensory functioning in persons with disabilities. Cochlear implants have effectively restored hearing in individuals with profound hearing loss or deafness. These implants facilitate sound perception by circumventing impaired sections of the ear and activating the auditory nerve. Retinal implants have shown promise in recovering vision for some forms of blindness by activating the optic nerve or visual cortex. Augmenting cognitive faculties Neural implants provide significant promise for augmenting cognitive capabilities. Researchers are exploring the use of brain implants to enhance memory, attention, and learning capabilities. By stimulating certain brain areas or networks, these implants may boost memory creation and retrieval, improve attentional concentration, and expedite learning. These discoveries may have profound consequences for education, rehabilitation, and the treatment of cognitive illnesses such as Alzheimer's disease. Regulating prosthetic extremities brain implants are essential for the development of sophisticated prosthetic limbs that can be operated directly via brain impulses. Neuroprosthetics provide a communication interface between the user's brain and the prosthesis, allowing for more intuitive and natural motions. Neural implants may interpret the user's intention to move and convert those signals into instructions that govern the motions of the prosthetic limb. This technology has enabled amputees to restore capability and autonomy, with continuous research focused on enhancing these systems.

Keywords: *neuroprosthetics, groundbreaking, enhancement, stimulation.*

Introduction

Neural interface recording and stimulation has shown to be a useful diagnostic and therapeutic approach for several neurological conditions. Modern brain probes, emphasizing the development of closed-loop systems, must integrate both functions while accommodating the varied design specifications for distinct electrode types, potentially including diverse modalities for each function. Consequently, there has been significant development in this study domain, accompanied by

[1,2,3,4]International School Of Technology And Sciences For Women, A.P, India.

some unique and promising advancements in neural probe design. 2 Bioelectronic medicine is an emerging discipline that aims to develop novel brain stimulation techniques while pursuing two primary objectives: to minimize adverse effects on patients and to address technical challenges related to existing brain implant designs. With the advancement of these technologies, the applications for brain stimulation have proliferated, currently covering a broad spectrum of neurological and mood diseases, including Parkinson's disease (PD) and depression. Despite the decreasing mortality rates associated with conditions like epilepsy and Parkinson's disease, a unified effort is necessary to enhance patients' quality of life, particularly in terms of disability-adjusted life years. Innovative neurotechnologies aimed at capturing and stimulating brain activity may reduce the strain on patients and their caretakers. The recent focus on adaptable, smaller brain probes has influenced the newest generation of implant design. By improving every stage of probe design and manufacture, resilient and creative brain probes will be developed for the future of patient care.

This progress report examines the history of brain implants, including the latest successful methodologies and their evolution from initial technology. Recent advancements in tissue-like materials and mesh electronics have significantly improved the design and dimensions of brain probes. To avert an immune reaction, the probes must replicate the flexibility, softness, and micron-scale characteristics of the target organs or tissues. Nevertheless, these attributes provide a difficulty for implantation: a balance must be established between flexibility and rigidity throughout the procedure to limit superfluous tissue injury. A completely flexible probe necessitates the removal of a potentially extensive section of the skull and dura mater, which may impede the healing process. Despite advancements in probe design beyond conventional silicon, wired probes will always face limitations, hindering their seamless integration with tissue. Wireless, batteryless power constitutes a significant obstacle for continuous implantation and advancement to clinical use.

Observations

Four individuals had bilateral implantation of the Summit RC+S bidirectional neural interface, connected to quadripolar depth leads in the subthalamic nuclei and subdural paddle-type leads across the major motor and sensory cortices. All participants had idiopathic Parkinson's disease characterized by motor fluctuations, including significant bradykinesia and stiffness during off-medication periods, but differed in the severity of off-period tremor and on-period dyskinesia (Table 1). Data were gathered during the first 1-3 months post-surgery using wireless transmission of multichannel field potentials to an external computer, both at home and at the clinic. (**Figure 1**).

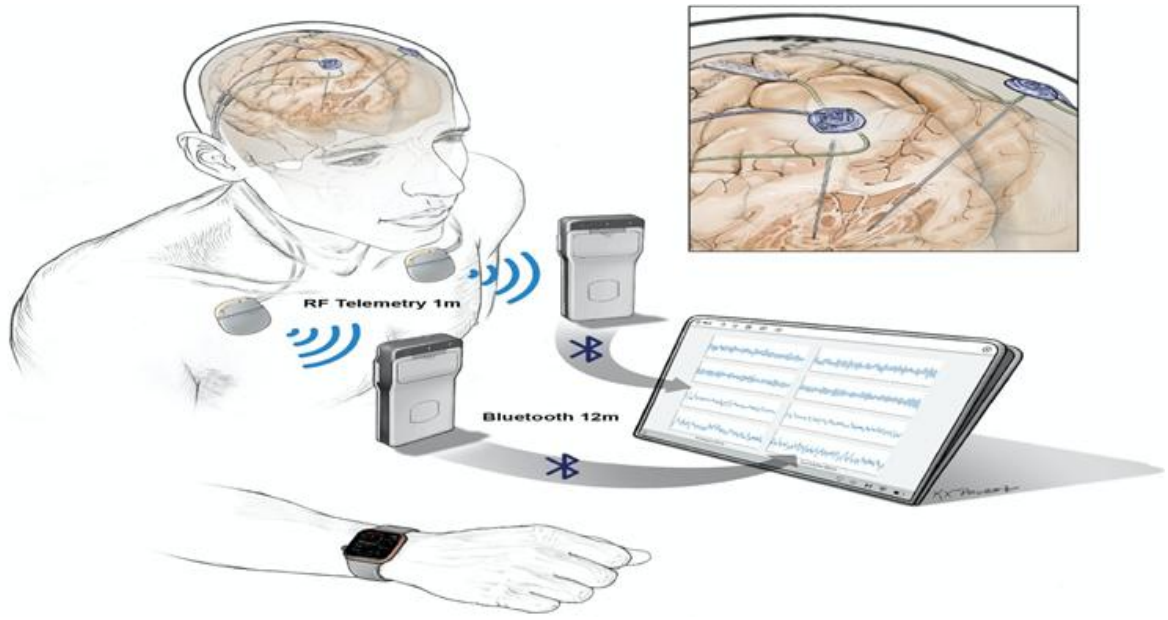

Figure 1. Configuration of implanted hardware and method of data streaming.

Quadripolar leads were bilaterally implanted into the subthalamic nuclei and positioned in the subdural region above the precentral gyri (the inset offers a magnified perspective). Each DBS lead and cortical paddle pair were interconnected by tunneled lead extenders to the ipsilateral Summit RC+S bidirectional implanted device.

Implantable pulse generator (IPG) situated in a pocket above the pectoralis muscle. Each RC+S employs radiofrequency telemetry within the medical implant communication spectrum (MICS) band to wirelessly transmit data to a compact relay device typically worn by the patient. The relay devices communicate via Bluetooth with a compact Windows-based tablet at a range of up to 12 meters, enabling the detection of local field potentials from a maximum of four bipolar electrode pairs for up to 30 hours per implantable pulse generator before recharging is required. The tablet's custom software enables remote modification of device streaming settings or adjustment of integrated adaptive DBS algorithms from home. An actigraphy monitor resembling a wristwatch is uploaded to a server that is offline synced with neural recordings for the purpose of analyzing brain-behavior connections. Precise lead placement was confirmed by intraoperative physiological recordings (Figure 2 a,b) and physically via postoperative CT scans computationally merged with preoperative MRI scans (example lead placements in Figure 2c; lead locations for all patients are detailed in Table S1). Therapeutic continuous subthalamic nucleus neurostimulation (standard clinical treatment) commenced one month after implantation. No significant adverse events were associated with the procedure or the trial regimen.

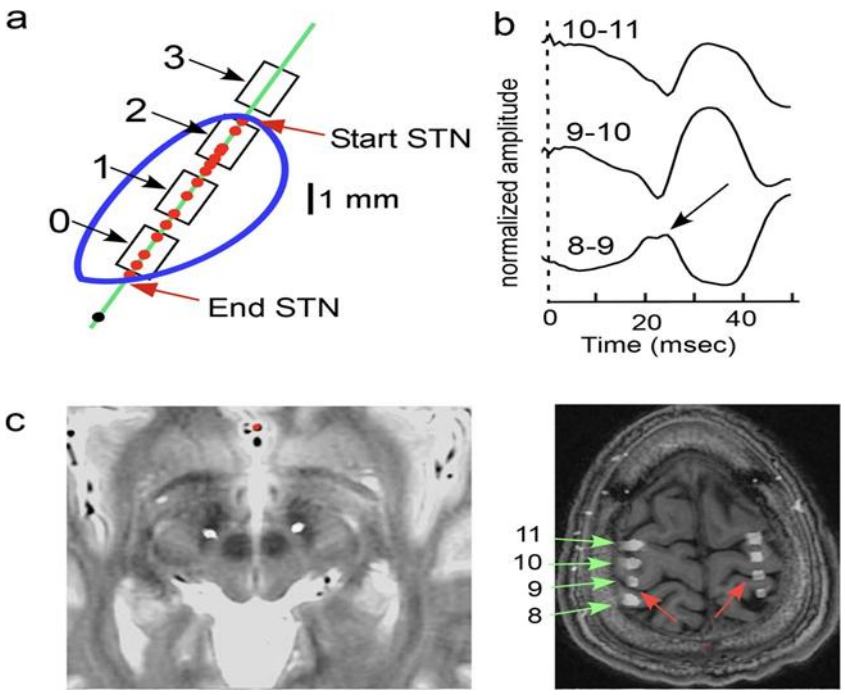

Figure 2. **Anatomic and physiological localization of subthalamic and cortical leads**

(example from RCS04). **a**, Localization of STN connections in relation to the boundaries of STN (highlighted in blue) as determined by microelectrode mapping. The microelectrode map (green line) delineates the boundaries of the STN, as identified by cells (red dots) exhibiting characteristic single-unit discharge patterns and rates of the STN. The map delineates the prescribed depth for the DBS lead, with contact numbers clearly shown. The central connections (1 and 2) are located within the dorsal 4 mm of the subthalamic nucleus (motor region). The dark dot represents a cell in the substantia nigra, pars reticulata. Somatosensory evoked potential, elicited by median nerve stimulation, recorded from the subdural paddle lead and montaged for three overlapping contact pairings. The reversal of the N20 potential between pairings 8-9 and 9-10 (shown by the arrow) demonstrates the localization of contact 9 to the main motor cortex, corroborating future imaging

findings. c, Position of the leads from postoperative CT computationally integrated with the preoperative planning MRI. The left subthalamic nucleus (STN) is prominent on axial T2-weighted MRI, appearing as an area of T2 hypointensity. Quadripolar subdural paddle connections in axial T1-weighted MRI illustrating their proximity to the central sulcus (red arrows) and the enumeration of contacts (green arrows).

Data attributes, movement-related activities, and the impact of levodopa in clinical settings. Data were collected in the clinic three weeks post-implantation to assess recording quality, the existence of movement-related activity, and the effects of levodopa in specified on/off states.

Four-channel time series recordings were conducted on each side, including two cortical and two subthalamic channels (Figure 3a). In the sensorimotor cortex, the commencement of movement correlated with a typical decrease in beta band activity, followed by a rise in broadband activity within the 50-200 Hz range, indicating local cortical activation. (**Figure 3b**).

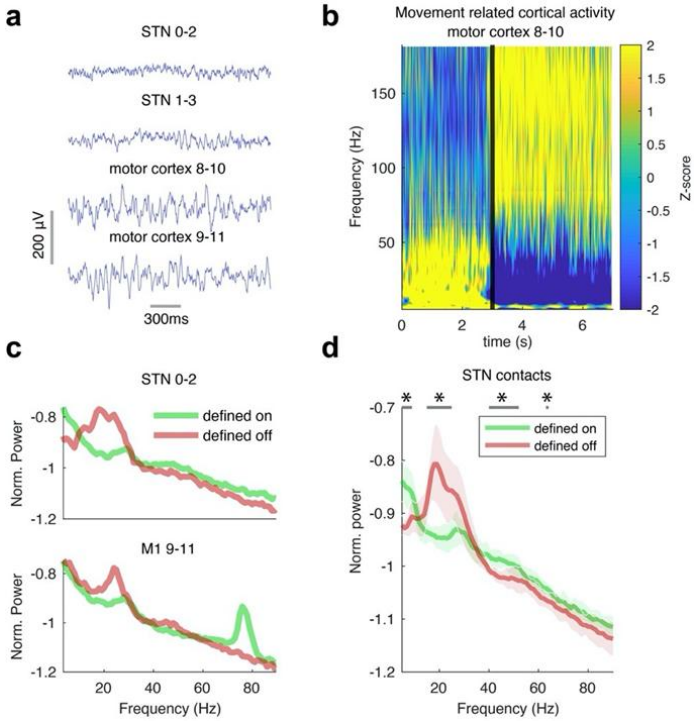

Figure 3. **Data examples and demonstration of effects of movement and levodopa in-clinic.**

aExample field potentials obtained from the right hemisphere, with cortical data shown above and STN data below.

The horizontal gray line at the bottom left indicates 300 milliseconds, while the vertical line represents 100 microvolts. Example spectrogram of ECoG activity (bipolar recordings from contacts 8-10) illustrating a canonical decrease in movement-related alpha and beta bands (8-35 Hz) and an increase in broadband activity (50-200 Hz), consistent with placement over the sensorimotor cortex (from RCS04), recorded 27 days post-implantation at a sampling rate of 500 Hz. The dotted vertical line signifies the commencement of movement. The color scale is standardized using z-scores. Example power spectra of STN and motor cortex field potentials illustrating the oscillatory profiles of off-levodopa (red) and on-levodopa (green) states (patient RCS01), derived from 30-second recordings. The amplitude of STN beta is consistently diminished in the on-medication condition. $p < 0.001$. Average PSD plots over both hemispheres, both recording montages, and all four patients (average shown by a black line, with the shaded region indicating one standard deviation). The horizontal bar illustrates frequency regions that exhibited large disparities across states. Antiparkinsonian dopaminergic agents, such as levodopa, are believed to elicit significant alterations in oscillatory activity within the basal

ganglia, as shown by prior perioperative recordings in humans using externalized brain leads. Consequently, we gathered data under specified pharmacological conditions: after a 12-hour cessation of antiparkinsonian drugs ("off"), and subsequent to a suprathreshold administration of levodopa/carbidopa ("on"). The medicated condition correlated with the anticipated decrease in subthalamic beta band (13-30 Hz) activity in each individual instance (Figure 3c) and across all 16 subthalamic recordings ($p < 0.001$, Generalized Estimating Equations (GEE)) (Fig 3d). The acute effects of levodopa previously noted using externalized leads were corroborated by wireless data transmission from an implanted device, recorded 2-4 weeks post-surgery. In individuals exhibiting significant dyskinesias, a motor cortex oscillation at 60-90 Hz was seen during the on-state12 (Figure 3c).

Physiological markers of motor symptoms found by the integration of at-home brain recordings and wearable devices.

A problem in invasive human brain recordings is the confirmation of results from acute in-hospital recording paradigms in chronic settings when patients engage in regular activities. Patients transmitted eight channels of brain data from home for a cumulative duration of 548 hours, while undergoing their usual on/off variations related to their standard regimen of antiparkinsonian drugs, including during sleep. Data were gathered 2-4 weeks post-device implantation, before commencing conventional therapeutic neurostimulation. Clinically approved bilateral wrist-mounted wearable monitors (Parkinson's KinetiGraph (PKG) watch) delivered numerical ratings for bradykinesia and dyskinesia every 2 minutes, derived from a 10-minute moving average (Figure 4a). All patients had motor fluctuations, as shown by their PKG monitor data, with periodic score swings similar to those in Figure 4a.

Neural data were evaluated in 10-minute intervals to align with the duration during which motor scores were derived from the PKG wearable device. A power spectrum was computed for each 10-minute segment and overlaid for all individual site recordings among individuals (Figure S1). Sleep stages, as indicated by PKG scores, often exhibited significant delta activity in both the STN and cortex (Figure S1). For awake data, the power spectra derived from 10-minute intervals were then categorized into mobile ("estimated on") and immobile ("estimated off") segments based on PKG scores and averaged. A time-frequency study conducted over a single day (7.5 hours) from one participant indicates that transitions between on and off states correlate with concurrent fast shifts in beta and gamma band oscillatory activity, as well as in coherence between the STN and cortex (Figure 4b). Mean LFP power spectrum

The data separated by the wearable monitor (42.7 hours of recording) substantially reflects the patterns identified in specified on/off states during clinical evaluations: A notable STN beta band peak is seen while off, which vanishes during on states, with a significant motor cortex gamma band peak at 75 Hz during on states with dyskinesia (Figure 4c, compare to short in-clinic recordings in Figure 3c).

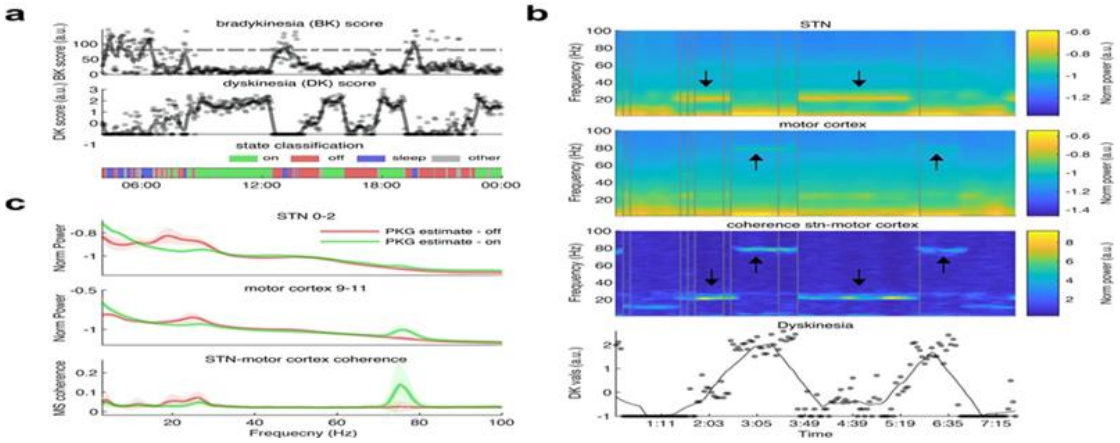

Figure 4. Decoding motor fluctuations from long duration recordings at home, single subject example (RCS01).

a, Data from the wearable Personal KinetiGraph (PKG) monitor provides ratings for bradykinesia and dyskinesia at 10-minute intervals. Illustration from one day. The assignment of state is shown in the bottom bar. Documenting transitions between immobile (off) and mobile/dyskinetic (on) states. Top spectrograms for the subthalamic nucleus (STN) and motor cortex, together with STN-motor cortex coherence, during a duration of 7.5 hours (all times PM). Arrows denote frequency zones responsive to on-off variations. The grey vertical lines indicate regions when the recording was interrupted and subsequently concatenated. The PKG dyskinesia scores reflect four transitions between off (low dyskinesia) and on (high dyskinesia) states. These are linked to transitions in beta and gamma oscillatory activity. Power spectra of the subthalamic nucleus (STN) and motor cortex, together with STN-motor cortex coherence, for all awake data from patient RCS01, classified by mobile and immobile states (as determined by PKG) and averaged. Shaded error bars denote one standard deviation.

The coherence between the STN and motor cortex differentiated on and off states (Figure 4c), indicating the involvement of basal ganglia-cortical oscillatory interactions, alongside individual oscillatory profiles, in the identification of motor function from neural recordings. Variations in these spectral patterns across different participants were observed, aligning with inter-subject differences in their most salient motor indications (Figure S1). For instance, in the person exhibiting significant off-period tremor (RCS03), an oscillation at double the tremor frequency was seen, particularly in STN-cortical coherence, during tremor episodes (Figure S1). This physiological hallmark of tremor has already been identified in the brain by magnetoencephalography.

Figure 5a illustrates the amount of hours of data transmitted at home by each patient. In all patients, considerable neuronal data separation between estimated on and estimated off states was seen in the STN beta band and cortical gamma band. (**Figure 5b**).

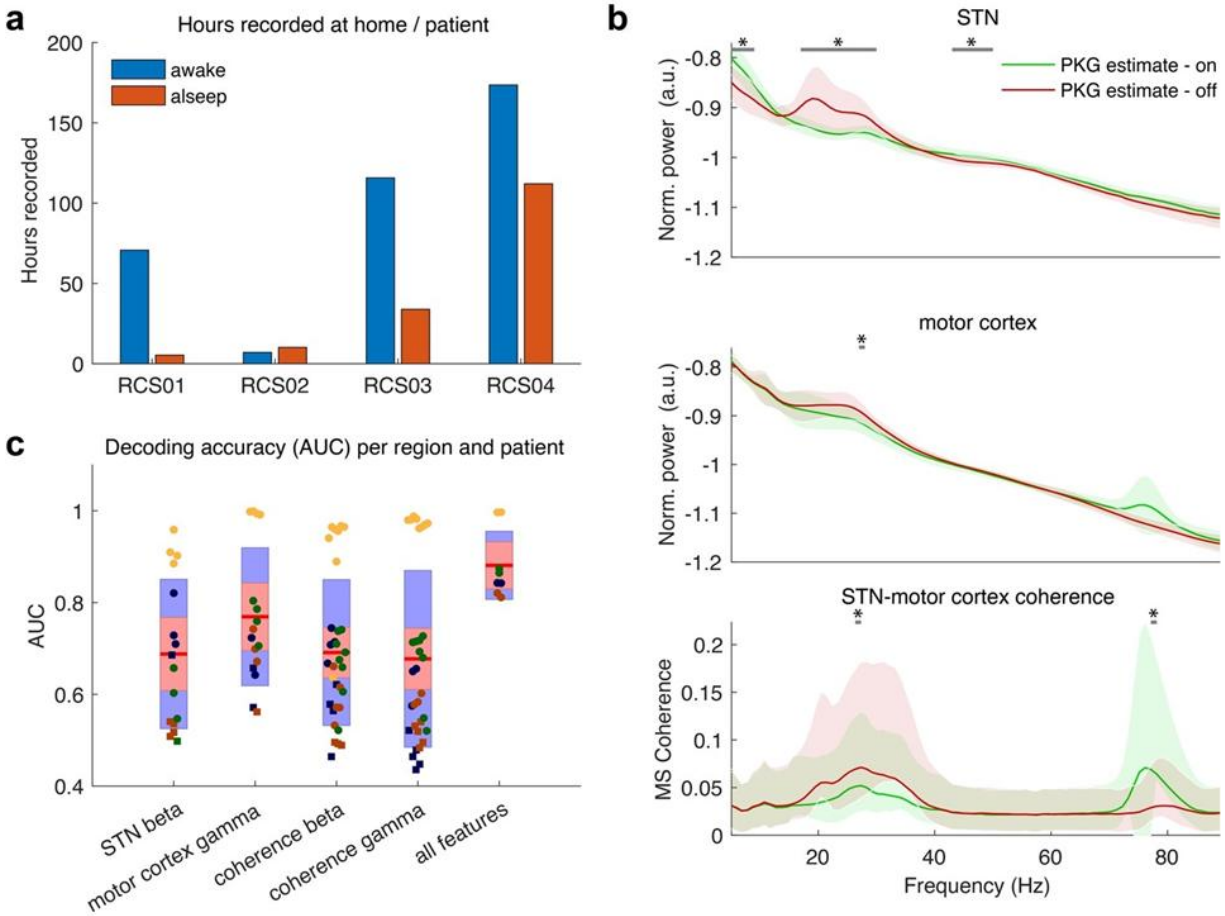

Figure 5. Decoding motor fluctuations from long duration recordings at home, group data.

aNumber of hours documented by each patient, power spectra of the subthalamic nucleus and motor cortex, and coherence between the subthalamic nucleus and motor cortex, for home recordings aggregated over all individuals. Horizontal bars with asterisks indicate frequencies that varied across states after adjustment for multiple comparisons. Comparisons indicate that the area under the curve (AUC) from ROC (receiver operating characteristic) analysis demonstrates that including data from both the STN and cortex more effectively distinguishes between mobile and immobile states, as categorized by PKG scores, than each location alone. The input for each ROC curve (a singular point on the graph) was derived by calculating the average beta band spectral power from the STN (for each patient, side, and two potential contact pairs - resulting in 16 points), average gamma power from the cortex, or a synthesis of estimates across recording montages (two values from the STN and two from the cortex). The four colors represent the four academic disciplines.

The specificity and sensitivity of these neural markers for decoding on and off behavioral states were assessed across all recordings from all participants using receiver operating characteristic curve (ROC) analysis (Figure 5c). Discrimination between on and off states was achievable using either STN beta activity (Area Under Curve (AUC) range 0.5-0.96) or motor cortex gamma activity (AUC range 0.56-1). A significant controversy in the field of behavioral state decoding from brain recordings concerns the use of subcortical data, cortical data, or a combination of both. The integration of subcortical and cortical data yielded optimal behavioral discrimination (AUC range 0.81-1.0) (Figure 5c), highlighting the efficacy of multisite sensing for bidirectional interfaces. The importance of decoding was evaluated within participants non-parametrically by randomizing the "on" and "off" labels and doing 5-fold cross-validation repeatedly. Single-site spectral power in the beta or gamma bands during ten-minute recordings predicted motor states in most, but not all, hemispheres. However, when both recording sites were integrated and cortex-STN coherence was considered, ten-minute segments of neural data effectively differentiated on and off states across all hemispheres (Figure 5c).

Unsupervised grouping of brain data to identify discrete behavioral states.

A primary objective for the therapeutic use of bidirectional interfaces in neurology and psychiatry is the deployment of adaptive deep brain stimulation (DBS), using electrophysiological signatures (biomarkers) indicative of certain indications and symptoms. Four, fifteen, nineteen. To do this effectively when biomarkers are highly customized, discrete brain states must be discernible by "unsupervised" clustering algorithms, which classify neural data without reliance on linked behavioral monitors, patient self-reports, or physician assessments. We used a density-based clustering algorithm for unsupervised grouping of data points in dimensionality-reduced power spectra20 (Figure 6a). We choose this approach since it does not need specifying the number of states, in contrast to k-means clustering. Unsupervised clustering methods successfully identified clusters that aligned with supervised clustering (on/off state estimations grouped by wearable PKG monitor) with significant concordance (mean 74%, range 59%-89%). Density-based clustering achieved a mean of 74.5%, with a range of 59% to 90% for template-based clustering (Figure 6c). A secondary clustering approach utilizes the power spectra from short in-clinic recordings, conducted during certain behavioral states, as "templates" for unsupervised grouping of home data ("template-based clustering," Figure 6b). In illnesses where behavioral states may be easily created in a clinical setting, our approach effectively identifies such states in home recordings. Template clustering demonstrates significant concordance with supervised clustering for STN data.

(**Figure 6c**).

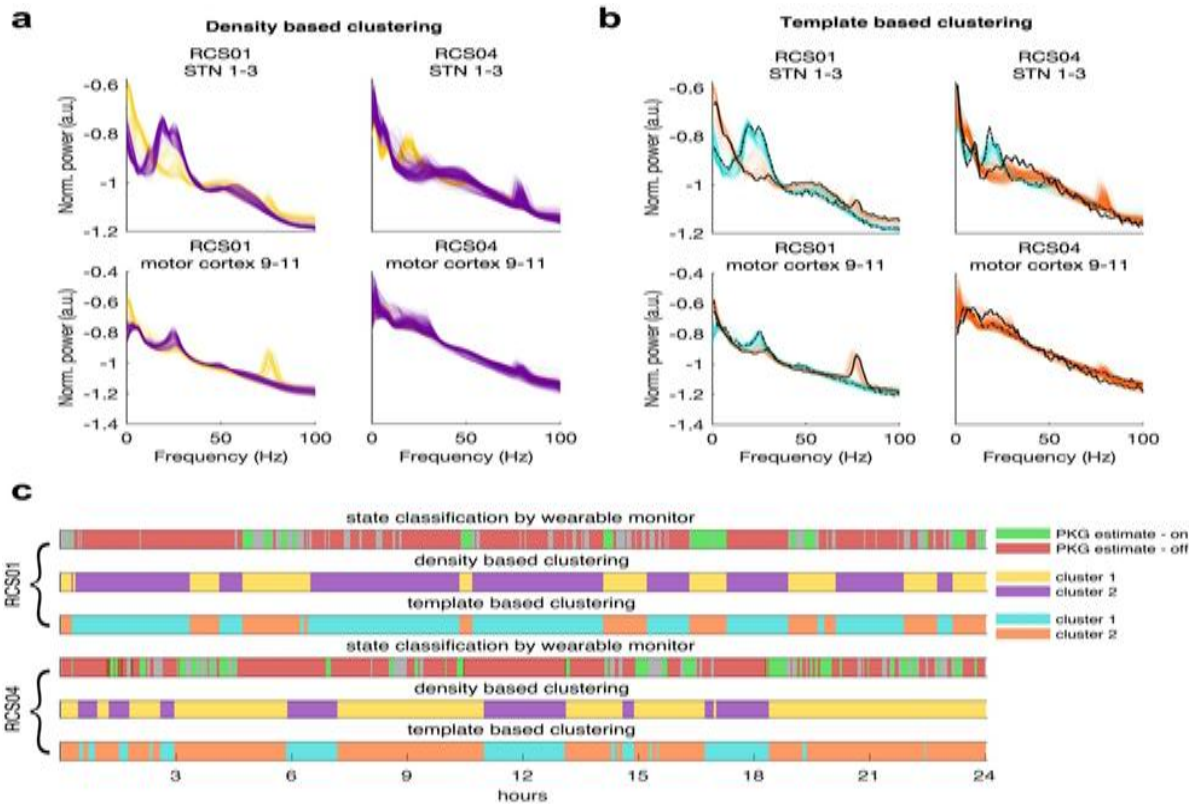

Figure 6. Unsupervised clustering segregates neural data into specific behavioral states. Examples patients are RCS01 and RCS04.

All raw data (recorded in the awake state) were segregated using unsupervised clustering algorithms with two different paradigms: **a,** Unsupervised clustering using the density based method of Laio[20]. **b,** Clustering of PSDs based on template PSDs from in clinic recording in defined on/off medication states. Black lines are the

template PSD's (dotted = off medication, solid = on medication). **c,** Concordance between brain states derived from unsupervised and supervised clustering methods (24 hour data sample, STN only). Barcodes compare motor state estimates derived from the wearable monitors, with the clusters derived from type of clustering algorithm.

Advanced device features that enable embedded adaptive stimulation

A primary problem in the development of implanted bidirectional neural interfaces is facilitating sensing from the same array used for therapeutic stimulation, an essential function for adaptive neurostimulation. This is especially difficult with subcortical targets, since the amplitude of field potentials from non-layered structures is often <10 µV, which is 5 to 10 times lower than those recorded from the cortical surface. Prior bidirectional interfaces often permitted significant sensing just during intervals of absence stimulation or necessitated sensing from a remote electrode array, such as a cortical array during subcortical stimulation. Utilizing a "sandwiched" sensing configuration to exploit common mode rejection (bipolar sensing from the contacts flanking a monopolar stimulating contact), we demonstrate that chronic therapeutic stimulation diminishes STN beta power, without a corresponding alteration in cortical beta power (Fig 7a). Violin graphs illustrate the impact of persistent stimulation on the variability of STN beta band activity (Fig 7b). Before therapeutic treatment, the beta amplitude range has a bimodal distribution, reflecting on- and off-states. Chronic therapeutic DBS eradicates pathologically heightened beta epochs while maintaining variability of beta band activity within a reduced range. The maintenance of task-related variability in beta activity may be crucial for proper mobility during DBS22.

An encouraging although technically challenging method for adaptive DBS involves using brief sequences of DBS activated by bursts of oscillatory activity, aimed at reducing the length of pathologically extended bursts. This method has shown superior effectiveness in Parkinson's disease compared to conventional continuous stimulation; nevertheless, it has only been used with externalized leads linked to external amplifiers and computers, or with implanted devices transmitting to an external computer in a "distributed mode." Consequently, we evaluated this technique for adaptive DBS within a fully integrated framework (Figure 7c). A prevalent drawback of feedback control systems is the emergence of "limit cycles," characterized by extremely regular oscillatory behavior where each state alteration induces an opposing change, resulting in the detector's inadequate response to variations in brain activity. Erratic fluctuations in detector state indicate suitable algorithm efficacy without settling into a limit cycle (arrow in **Figure 7c**).

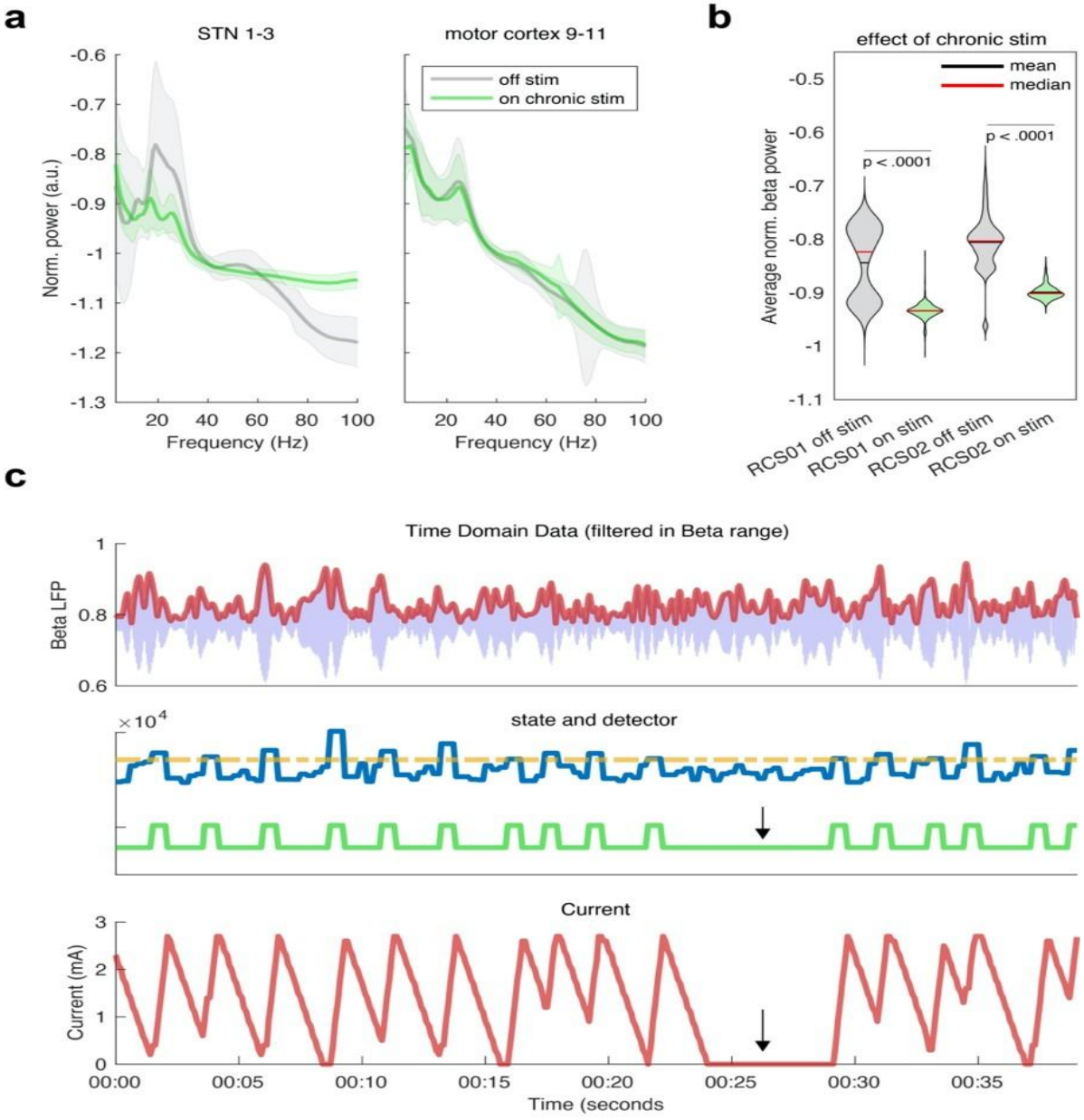

Figure 7. **Recording during therapeutic DBS, and demonstration of adaptive DBS.**

a, Continuous recording from the same quadripolar subthalamic nucleus contact array used for therapeutic stimulation. Illustration from RCS01. Mean PSDs for 10-minute data segments categorized by off Stimulation (grey) and on stimulation (green) for a cumulative 87.5 hours of home recording. Violin plots illustrating the average beta power (5Hz window encompassing the peak)

during chronic stimulation in two rigid/akinetic patients, both on and off stimulation. Chronic STN DBS eradicates episodes of abnormally heightened STN beta band activity, although maintains variability within a reduced range (the median during stimulation contrasts with that before stimulation cessation). An example of an integrated adaptive deep brain stimulation algorithm intended to activate in response to beta bursts. The upper panel displays filtered STN time domain data (blue) within the beta region (17-19Hz), focused on the subject-specific beta peak, with amplitude (Hilbert transform, red) overlaid. The middle panel displays the threshold used for the algorithm (shown by the dotted orange line) alongside the detector (in blue), which represents a smoothed estimate of instantaneous beta power.
The algorithm's status is shown as green, wherein the detector is in a "high" state when it surpasses the line and in a "low" condition when it falls below the line. Lower panel shows present amplitude in milliamperes. This technique is intended to "trim" beta bursts as proposed by Little et al. (2013). Upon detection of a beta burst, stimulation is swiftly escalated, followed by a quick reduction after the burst diminishes. The arrow denotes a 5-second interval during which the detector remains untriggered.

Discussion

This paper presents the first human use of an implanted bidirectional neural interface engineered for prolonged wireless transmission of brain signals during routine everyday activities at home. In four Parkinson's disease patients with bilateral implantation of motor cortex and basal ganglia leads, we demonstrate that oscillatory activity patterns in both structures can decode hypokinetic and hyperkinetic states, as evidenced by correlating the recordings with wearable monitors that track these motor fluctuations behaviorally. We demonstrate that brain states may be differentiated using an unsupervised clustering technique applied to the power spectra of brief data segments, offering an expedited approach for tailored biomarker identification. We ultimately showcase the technological capabilities of devices that have not been easily attainable in implantable sensing systems: sensing during stimulation from neighboring contacts of a multipolar array, and integrated adaptive deep brain stimulation using minor subcortical signals for regulation.

Conclusion

In recent years, neural devices have transitioned from rigid, wired implants, like the Michigan probe, to smaller, flexible, and innovative geometries to promote effective chronic recording and stimulation. By considering the properties of brain tissues, meticulous design, production, and implantation techniques have produced a new generation of devices that show encouraging outcomes in animal studies. Particularly, methodologies like NeuE and mesh electronics emulate soft tissue, facilitating integration with cells. To accomplish this, biocompatible, flexible substrates and encapsulating materials are used. The Young's modulus of these materials is often an order of magnitude lower than that of silicon, although it remains inferior to that of the brain. Although these substrates are generally appropriate for conventional cleanroom patterning and etching, methods like as transfer printing may be used to enhance device performance. This adaptability facilitates the use of diverse stimulation techniques, notably the new use of optogenetic probes with μ-LEDS. Ultimately, to achieve really implanted devices, wireless power transmission is essential to avoid recurrent operations, disrupt the device and its adjacent tissues, and transcend dependence on battery-operated medical implants. Ongoing research advancements suggest the feasibility of integrating these innovative, advanced implants into clinical practice to treat patients with neurological disorders and provide superior future options.

References

[1] Lozano, A. M. *et al.* Deep brain stimulation: current challenges and future directions.

[2] *Nature reviews. Neurology* **15**, 148-160, doi:10.1038/s41582-018-0128-2 (2019).

[3] Brittain, J. S. & Brown, P. Oscillations and the basal ganglia: motor control and beyond.

[4] *NeuroImage* **85 Pt 2**, 637-647, doi:10.1016/j.neuroimage.2013.05.084 (2014).

[5] Starr, P. A. Totally Implantable Bidirectional Neural Prostheses: A Flexible Platform for Innovation in Neuromodulation. *Front Neurosci* **12**, 619, doi:10.3389/fnins.2018.00619 (2018).

[6] Sun, F. T. & Morrell, M. J. The RNS System: responsive cortical stimulation for the

treatment of refractory partial epilepsy. *Expert review of medical devices* **11**, 563-572, doi:10.1586/17434440.2014.947274 (2014).

[7] Rouse, A. G. *et al.* A chronic generalized bi-directional brain-machine interface. *Journal of neural engineering* **8**, 036018, doi:10.1088/1741-2560/8/3/036018 (2011).

[8] Swann, N. C. *et al.* Chronic multisite brain recordings from a totally implantable bidirectional neural interface: experience in 5 patients with Parkinson's disease. *Journal of neurosurgery* **128**, 605-616, doi:10.3171/2016.11.JNS161162 (2018).

[9] Stanslaski, S. *et al.* A Chronically Implantable Neural Coprocessor for Investigating the Treatment of Neurological Disorders. *IEEE transactions on biomedical circuits and systems* **12**, 1230-1245, doi:10.1109/TBCAS.2018.2880148 (2018).

[10] Kremen, V. *et al.* Integrating Brain Implants With Local and Distributed Computing Devices: A Next Generation Epilepsy Management System. *IEEE journal of translational engineering in health and medicine* **6**, 2500112, doi:10.1109/JTEHM.2018.2869398 (2018).

[11] Wozny, T. A. *et al.* Effects of hippocampal low-frequency stimulation in idiopathic non-human primate epilepsy assessed via a remote-sensing-enabled neurostimulator. *Experimental neurology* **294**, 68-77, doi:10.1016/j.expneurol.2017.05.003 (2017).

[12] Little, S. *et al.* Adaptive deep brain stimulation in advanced Parkinson disease. *Annals of neurology* **74**, 449-457, doi:10.1002/ana.23951 (2013).

[13] Little, S. *et al.* Adaptive deep brain stimulation for Parkinson's disease demonstrates reduced speech side effects compared to conventional stimulation in the acute setting. *Journal of neurology, neurosurgery, and psychiatry* **87**, 1388-1389, doi:10.1136/jnnp- 2016-313518 (2016).

[14] Swann, N. C. *et al.* Gamma Oscillations in the Hyperkinetic State Detected with Chronic Human Brain Recordings in Parkinson's Disease. *J Neurosci* **36**, 6445-6458, doi:10.1523/JNEUROSCI.1128-16.2016 (2016).

[15] de Hemptinne, C. *et al.* Exaggerated phase-amplitude coupling in the primary motor cortex in Parkinson disease. *Proceedings of the National Academy of Sciences of the United States of America* **110**, 4780-4785, doi:10.1073/pnas.1214546110 (2013).

[16] Silberstein, P. *et al.* Cortico-cortical coupling in Parkinson's disease and its modulation by therapy. *Brain* **128**, 1277-1291 (2005).

[17] Lo, M. C. & Widge, A. S. Closed-loop neuromodulation systems: next-generation treatments for psychiatric illness. *International review of psychiatry* **29**, 191-204, doi:10.1080/09540261.2017.1282438 (2017).

[18] Crone, N. E., Miglioretti, D. L., Gordon, B. & Lesser, R. P. Functional mapping of human sensorimotor cortex with electrocorticographic spectral analysis. II. Event-related synchronization in the gamma band. *Brain* **121 (Pt 12)**, 2301-2315 (1998).

[19] Horne, M. K., McGregor, S. & Bergquist, F. An objective fluctuation score for Parkinson's disease. *PloS one* **10**, e0124522, doi:10.1371/journal.pone.0124522 (2015).

[20] Timmermann, L. *et al.* The cerebral oscillatory network of parkinsonian resting tremor.

[21] *Brain* **126**, 199-212 (2003).